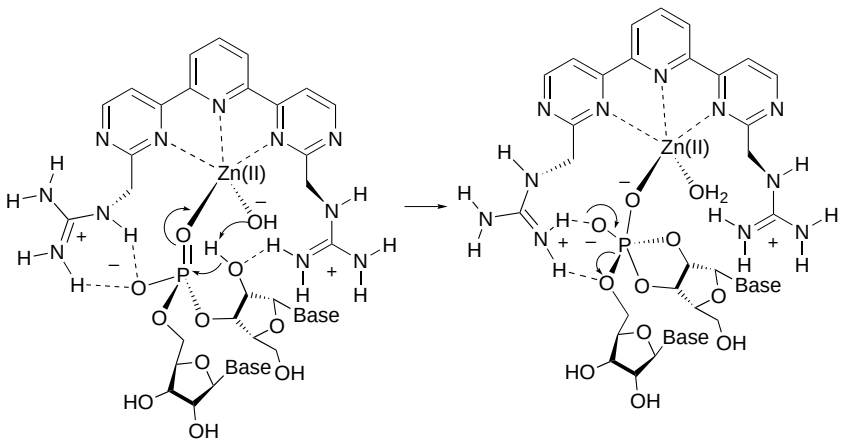

Scheme 2. Proposed mechanism for nucleophilic attack and leaving-group departure facilitated by **Zn^{II}-4**.

A possible mechanism (Scheme 2) for the hydrolysis of ApA by **Zn^{II}-4** includes double activation of the phosphate by coordination to the zinc center and to one of the guanidinium fragments, followed by Zn^{II}-OH general-base-promoted delivery of the 2′-OH group. Hence the guanidinium and ammonium arms are postulated to play several roles:[13] 1) to assist the binding of the phosphate group to the zinc ion, 2) to act as additional Lewis acids which polarize the phosphate group, 3) to lower the pK_a of a zinc-bound water molecule, and 4) potentially to protonate the leaving group.

In summary, a general strategy used by natural metallonucleases is to achieve the hydrolysis of phosphodiesters by cooperation between metal centers and amino acid residues. By creating a cleft that ensures guanidinium or ammonium groups and a zinc ion are proximal to one another, and preorganized to form contacts with a bound phosphodiester, we discovered cooperativity between the catalytic groups that is comparable to the enzyme SNase. The creation of other well-defined clefts wherein multiple productive contacts are made between catalyst and substrate may be anticipated to generate other efficient artificial enzymes.

Received: May 14, 2002 [Z19298]

[1] N. Sträter, W. N. Lipscomb, R. Klabunde, B. Krebs, *Angew. Chem.* **1996**, *108*, 2158; *Angew. Chem. Int. Ed. Engl.* **1996**, *35*, 2024; D. E. Wilcox, *Chem. Rev.* **1996**, *96*, 2435.

[2] D. M. Perreault, E. V. Anslyn, *Angew. Chem. Engl.* **1997**, *109*, 470; *Angew. Chem. Int. Ed. Engl.* **1997**, *36*, 432.

[3] E. H. Serpersu, D. Shortle, A. S. Mildvan, *Biochemistry* **1987**, *26*, 1289.

[4] C. A. Stein, J. S. Cohen, *Cancer Res.* **1988**, *48*, 2659; E. Uhlmann, A. Peyman, *Chem. Rev.* **1990**, *90*, 543.

[5] N. T. Bobby, A. T. Daniher, J. K. Bashkin, *Chem. Rev.* **1998**, *98*, 939; A. Blaskó, T. C. Bruice, *Acc. Chem. Res.* **1999**, *32*, 475; N. H. Williams, B. Takasaki, M. Wall, J. Chin, *Acc. Chem. Res.* **1999**, *32*, 485; G. Pratviel, J. Bernardou, B. Meunier, *Adv. Inorg. Chem.* **1997**, *45*, 251.

[6] For examples see: a) P. Molenveld, J. F. J. Engbersen, D. N. Reinhoudt, *Chem. Soc. Rev.* **2000**, *29*, 75; b) M. K. Stern, J. K. Bashkin, E. D. Sall, *J. Am. Chem. Soc.* **1990**, *112*, 5357; c) B. Linkletter, J. Chin, *Angew. Chem.* **1995**, *107*, 529; *Angew. Chem. Int. Ed. Engl.* **1995**, *34*, 472; d) S. Liu, Z. Luo, A. D. Hamilton, *Angew. Chem.* **1997**, *109*, 2794; *Angew. Chem. Int. Ed. Engl.* **1997**, *36*, 2678; e) M. Komiyama, N. Takeda, H. Shigekawa, *Chem. Commun.* **1999**, 1443; P. Molenveld, J. F. J. Engbersen, D. N. Reinhoudt, *Angew. Chem.* **1999**, *111*, 3387; *Angew. Chem. Int. Ed.* **1999**, *38*, 3189; f) K. A. Deal, A. C. Hengge, J. N. Burstyn, *J. Am. Chem. Soc.* **1996**, *118*, 1713; g) M. J. Young, J. Chin, *J. Am. Chem. Soc.* **1995**, *117*, 10577–10578; M. Komiyama, K. Yoshinari, *J. Org. Chem.* **1997**, *62*, 2155–2160.

[7] R. Breslow, D. Berger, D.-L. Huang, *J. Am. Chem. Soc.* **1990**, *112*, 3686; J. R. Morrow, D. Epstein *J. Chem. Soc. Chem. Commun.* **1995**, 2431; E. Kimura, Y. Kodama, T. Koike, M. Shiro, *J. Am. Chem. Soc.* **1995**, *117*, 8304; P. Molenveld, J. F. J. Engbersen, D. N. Reinhoudt, *J. Org. Chem.* **1999**, *64*, 6227–6341; Y. Baran, T. W. Hambley, G. A. Lawrance, E. N. Wilkes, *Aust. J. Chem.* **1997**, 883.

[8] E. Kövári, R. Krämer, *J. Am. Chem. Soc.* **1996**, *118*, 12704.

[9] M. Wall, B. Linkletter, D. Williams, A.-M. Lebuis, R. C. Hynes, J. Chin, *J. Am. Chem. Soc.* **1999**, *121*, 4710.

[10] J. Smith, K. Ariga, E. V. Anslyn, *J. Am. Chem. Soc.* **1993**, *115*, 362. For other studies using bisguanidinium receptors that are not as rigid see: V. Jubian, R. P. Dixon, A. D. Hamilton, *J. Am. Chem. Soc.* **1992**, *114*, 1120; M.-S. Muche, P. Kamalaprija, M. W. Gobel, *Tetrahedron Lett.* **1997**, *38*, 2923.

[11] Although **Zn^{II}-4** was originally designed by us to be an RNA hydrolysis catalyst, we have also reported its use as a selective receptor for aspartate in an indicator displacement assay. H. Aït-Haddou, S. L. Wiskur, V. M. Lynch, E. V. Anslyn, *J. Am. Chem. Soc.* **2001**, *123*, 11296.

[12] D. A. Usher, *J. Am. Chem. Soc.* **1970**, *92*, 4699. Another estimate places the half-life for uridylyl(3′→5′uridine (UpU) to be 100 years, which makes our estimated rate enhancement over the background rate even larger; N. H. Williams, B. Takasaki, M. Wall, J. Chin, *Acc. Chem. Res.* **1999**, *32*, 485.

[13] C. L. Hannon, E. V. Anslyn, *Bioorg. Chem. Front.* **1993**, *3*, 193.

Fabrication of Ultrafine Conducting Polymer and Graphite Nanoparticles**

Jyongsik Jang,* Joon H. Oh, and Galen D. Stucky

The ability to selectively tune defects, electronic states, and surface chemistry has motivated the development of a variety of methods to fabricate metallic,[1] inorganic,[2] and polymeric nanoparticles.[3] While metallic and inorganic semiconductor nanoparticles with dimensions of around 1 nm are routinely made, polymer nanoparticles with dimensions less than 5 nm have not been reported. Here we report the selective fabrication of amorphous polypyrrole (PPy) nanoparticles as small as 2 nm in diameter, using microemulsion polymer-

[*] Prof. Dr. J. Jang, J. H. Oh
Hyperstructured Organic Materials Research Center and
School of Chemical Engineering, Seoul National University
Shinlimdong 56-1, Seoul 151-742 (Korea)
Fax: (+82) 2-888-1604
E-mail: jsjang@plaza.snu.ac.kr
Prof. Dr. G. D. Stucky
Department of Chemistry and Biochemistry
University of California
Santa Barbara, CA 93106 (USA)

[**] This work was supported in part by the Brain-Korea 21 Program of the Korea Ministry of Education, by the Hyperstructured Organic Materials Research Center of Seoul National University, by the U.S. National Science Foundation (NSF), and by the Materials Research Laboratory Program of the NSF.

  0044-8249/02/4121-4016 $ 20.00+.50/0

ization[4] at low temperature. In addition, we also describe a novel fabrication of graphite nanoparticles with dimensions less than 2 nm, by using ultrasmall amorphous PPy as the carbon precursor. The amorphous PPy nanoparticles are transformed into ultrafine graphite particles in the presence of an iron complex dopant, which promotes the graphitization of amorphous PPy during carbonization. Our results show that the graphite nanoparticles, when blended with polycarbonate, have an improved transparent conducting performance compared with carbon nanotubes. Low-temperature microemulsion polymerization is found to be a versatile route for the production of a wide range of new polymer nanoparticles and can be expanded to the fabrication of metallic and inorganic nanoparticles by using the concept of "nanoreactors".

Cationic surfactants such as octyltrimethylammonium bromide (OTAB), decyltrimethylammonium bromide (DeTAB), and dodecyltrimethylammonium bromide (DTAB) were used to control the morphology of nanoparticles. Hexyltrimethylammonium bromide (HTAB) could not form highly ordered structures because of the weak hydrophobic interactions associated with short C_6 chains.[5] Surfactants with hydrocarbon chains longer than C_{16} were not suitable for low-temperature microemulsion polymerization because of their liquid-crystalline state and high viscosity. Pyrrole monomers were polymerized in micelles, using iron(III) chloride as the oxidant, at 3 °C. The ^{1}H NMR spectrum of the nanoparticles showed no methyl resonances, which might have originated from residual surfactants. FTIR spectroscopy showed PPy ring-stretching bands at 1469, 1485, and 1549 cm^{-1} and an N–H stretching band at 3403 cm^{-1}. Therefore, it is certain that the surfactants were removed and PPy was successfully synthesized. Energy-dispersive X-ray analysis (EDAX) indicated the presence of carbon (54.2 %), nitrogen (16.6 %), and iron (15.3 %). From these results, it is evident that the nanoparticles consist of PPy doped with an anionic iron complex.

Polymerization reactions using DeTAB (0.40 M) at 3 °C yielded PPy nanoparticles with an average diameter of approximately 2 nm, which was confirmed by high-resolution transmission electron microscopy (HRTEM) imaging and electron diffraction of the amorphous nanoparticles (Figure 1 a). To our knowledge, there are no reports describing the manufacture of any kind of polymeric nanoparticles with dimensions less than 5 nm[6] and this is the first experimental evidence for polymer nanoparticles in this size regime. Under these experimental conditions, PPy nanoparticles were fabricated between CMC I and CMC II (CMC = critical micelle concentration). This means that the product consisted mainly of PPy nanospheres. At room temperature the spherical nanoparticles were approximately 12 nm in diameter, while at 70 °C spherical mesoparticles (approximately 53 nm in diameter) were mainly obtained. As the polymerization temperature increases, the nanoparticle size also increases as a result of the increased mobility of surfactant chains. Figure 1 b presents the change in average particle size as a function of surfactant concentration at 3 °C. The size of the nanoparticles decreased with decreasing surfactant chain length. The enhanced flexibility of longer spacers provides more free volume inside the micelles and, therefore, larger particles. The

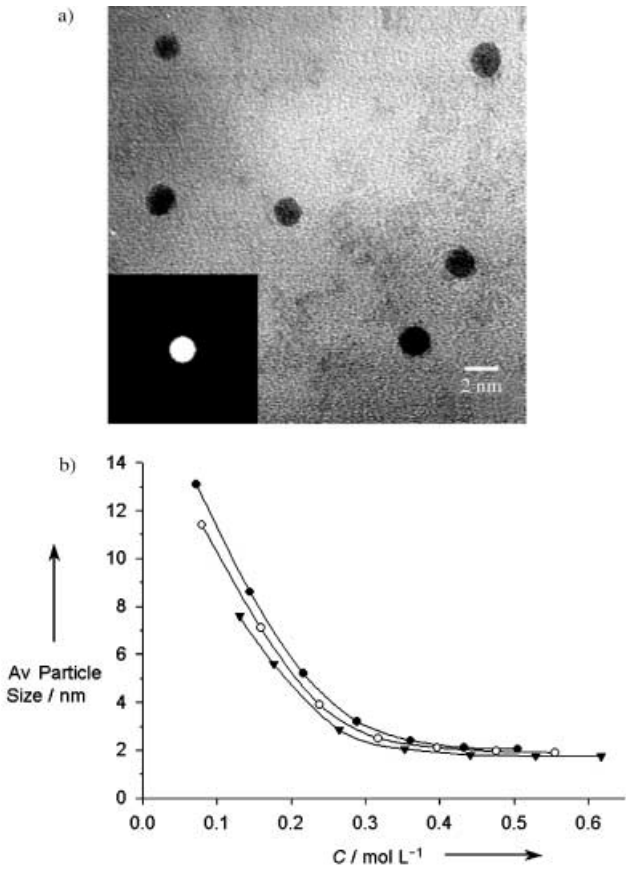

Figure 1. a) TEM image and nanobeam electron diffraction pattern of the PPy nanoparticles prepared using DeTAB (0.4 M) at 3 °C; b) Average change in nanoparticle size as a function of surfactant concentration (DTAB, ●; DeTAB, ○; OTAB, ▼). The average nanoparticle size was determined by TEM (50 particles counted).

micelle aggregation number (n) describes the number of surfactant molecules required to form a micelle; the value of n becomes smaller with shorter chain length.[7] Thus, the number of micelles increases with shorter spacer length at the same surfactant concentration, which results in a reduction in the particle size. As surfactant concentration increases, the nanoparticle size decreases and approaches an asymptotic value. The morphological transformation occurs over this concentration range as a result of the relative changes in interfacial and packing forces.

The amorphous PPy nanoparticles can be transformed into ultrafine graphite particles by carbonization. It has been reported that transition metals promote the formation of graphite during the carbonization process.[8] In our study, PPy nanoparticles were also synthesized by using ammonium persulfate as a comparative oxidant species. The control experiment showed that the doped iron complex anion facilitates the graphitization of PPy nanoparticles. For doped PPy nanoparticles, the loss of nitrogen atoms occurs between 400 and 600 °C, and carbonization reactions produce polycondensed aromatic hydrocarbons showing a high electrical conductivity.[9] When the PPy nanoparticles were carbonized above 750 °C, the conductivity was found to be higher than that of pure PPy nanoparticles, which is a consequence of the presence of graphitic species.

  0044-8249/02/4121-4017 $ 20.00+.50/0

Figure 2 shows a TEM image of carbonized PPy (CPPy) nanoparticles and their associated powder X-ray diffraction (XRD) pattern. The average particle size was 1.8 ± 0.4 nm, and the distribution was reasonably monodisperse; the carbonization temperature was 800 °C. The XRD pattern of CPPy confirms the presence of graphite in the nanoparticles, as the characteristic 002 and 100 Bragg reflections of graphenes are clearly displayed (Figure 2b). The electron diffraction pattern of CPPy nanoparticles also shows crystalline structure (Figure 2a). The degree of graphitization could be enhanced by treatment at higher temperatures. According to EDAX analysis, the graphite nanoparticles graphitized at 800 °C consist of carbon (73.8 %), nitrogen (1.3 %) and iron (8.6 %). The iron content could be removed without amorphization by heating the nanoparticles to reflux in nitric acid solution or by washing with excess methanol.

In general, powdered mixtures of vinyl polymers and metal oxides form graphite structures by heat treatment above 1000 °C.[10] Compared with carbonization at an elevated temperature, graphite formation occurs at a mild temperature under our experimental conditions. The microemulsion system increases the extent of the π-conjugation length and optimizes the arrangement of the molecular chains.[11] The size of polymer latex synthesized by microemulsion polymerization is much smaller than that synthesized by other synthetic methods. These effects probably bring about easier cyclization and mass-transfer flow during carbonization. Our novel methodology describes the first demonstration of the fabrication of ultrafine graphite particles using amorphous polymer nanoparticulate precursors with a metallic dopant.

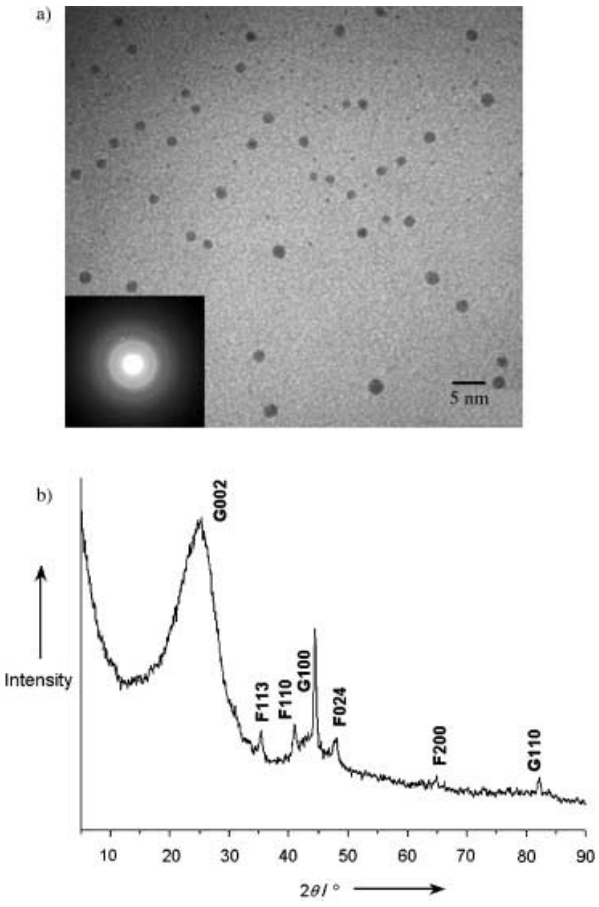

Figure 2. a) TEM image and nanobeam electron diffraction pattern of graphite nanoparticles fabricated by the carbonization of PPy nanoparticles prepared using DeTAB (0.4 M); b) powder X-ray diffraction pattern of the graphite nanoparticles (graphite, G; iron complex, F).

The ultrafine PPy and CPPy nanoparticles can be applied as optically transparent conducting materials. The PPy nanoparticles were blended with polycarbonate (PC), which is a typical transparent amorphous polymer used in glass substitutes and compact disks. Carbon nanofibers (CNs) are well-known as highly transparent conductive materials.[12] For a comparison, CNs were also mixed with PC. Figure 3 shows the transparency and conductivity of PC/CN, PC/PPy, and PC/CPPy films. The transparencies of PC/PPy and PC/CPPy films were much higher (up to 17 %) than that of PC/CN films at the same filler content (Figure 3a). To obtain a transparent film, conductive powders should have an average particle diameter no larger (approximately 0.2 μm) than half of the shortest wavelength of visible light.[12] As a consequence of their large diameter and high aspect ratio, CNs easily form bulky aggregates, which causes blackening of the as-prepared films. The conductivity of a PC/pure PPy film was slightly lower than that of a PC/CN film (Figure 3b). As mentioned above, the conductivity of the PPy nanoparticles can be enhanced by the carbonization process. The PC/CPPy film showed higher conductivity than the PC/CN film. As the filler content increases, the generation of local electronic paths is favorable to small and uniform CPPy fillers. Judging from these results, PC/CPPy films could be used as a substitute for indium–tin

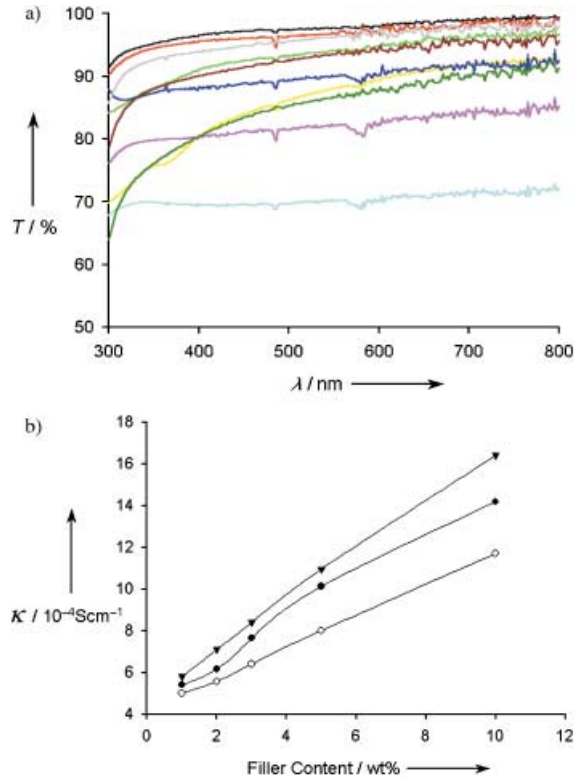

Figure 3. Transparency and conductivity of PC/CN, PC/PPy, and PC/CPPy films: a) Transparency (pure PC, black; PPy 1 wt %, red; PPy 3 wt %, green; PPy 10 wt %, yellow; CN 1 wt %, blue; CN 3 wt %, violet; CN 10 wt %, sky-blue; CPPy 1 wt %, gray; CPPy 3 wt %, brown; CPPy 10 wt %, deep-green); b) conductivity (PC/CN, ●; PC/PPy, ○; PC/CPPy, ▼).

  0044-8249/02/4121-4018 $ 20.00+.50/0 *Angew. Chem. Int. Ed.* **2002**, *41*, No. 21

oxide (ITO) as a potential transparent conducting material. In addition, CPPy nanoparticles could be applied as an anodic material in lithium-ion batteries because of their high conductivity and large surface area.

We have demonstrated a surfactant-mediated methodology for the synthesis of 2 nm spherical PPy nanoparticles. The carbonized PPy nanoparticles can be used as a highly transparent conductive material, which may possibly be a substitute for carbon nanofibers. Importantly, low-temperature microemulsion polymerization may provide a facile way to synthesize new polymer nanoparticles, and might be expanded to allow the fabrication of ultrafine metallic and inorganic particles, which embraces the concept of "nanoreactors".

Experimental Section

A variable amount of surfactant was magnetically stirred in distilled water (40 mL) at 3 °C. Pyrrole monomer (1.0 g, 14.9 mmol) was added dropwise to the surfactant solution, and iron(III) chloride hexahydrate (9.25 g, 34.3 mmol), dissolved in distilled water (5 mL), was added to the surfactant/pyrrole solution. Microemulsion polymerization proceeded while stirring for 3 h at 3 °C. The reaction product was placed in a separating funnel and excess methanol was added to remove the surfactants and the residual iron(III) chloride. The upper layer was discarded and the remaining nanoparticle precipitate was dried in a vacuum oven at room temperature.

The PPy nanoparticles were placed in a quartz tube in a furnace under N_2 atmosphere. The sample was heated to 800 °C at a heating rate of 3 °C min^{-1}, held at 800 °C for 5 h, and then cooled to room temperature.

PPy nanoparticles and PC were combined in THF. The mixed solution was spin-coated onto a glass slide using a PWM32 spinner (Headway Research, Inc.). Transparency of the films was measured with a UV/Vis spectrometer and the conductivity was determined by the van der Pauw method. As-prepared (AP)-grade CNs were purchased from Aldrich. PC/CN and PC/CPPy films were prepared by the same method. Film thicknesses were estimated with an Alpha-Step 500 surface profiler (Tencor). All films were approximately 270 nm thick, the growth being controlled by changing the spinning speed. TEM images were taken by a JEOL 2010 high-resolution microscope and EDAX analysis was carried out using a Philips CM 20 microscope.

Received: March 26, 2002
Revised: August 26, 2002 [Z18986]

[1] a) A. J. Zarur, J. Y. Ying, *Nature* **2000**, *403*, 65 – 67; b) A. K. Boal, F. Ilhan, J. D. Derouchey, T. Thurn-Albrecht, T. P. Russell, V. M. Rotello, *Nature* **2000**, *404*, 746 – 748; c) V. F. Puntes, K. M. Krishnan, A. P. Alivisatos, *Science* **2001**, *291*, 2115 – 2117.
[2] a) F. Caruso, R. A. Caruso, H. Möhwald, *Science* **1998**, *282*, 1111 – 1114; b) Y. Lu, H. Fan, A. Stump, T. L. Ward, T. Rieker, C. J. Brinker, *Nature* **1999**, *398*, 223 – 226.
[3] a) S. A. Johnson, P. J. Ollivier, T. E. Mallouk, *Science* **1999**, *283*, 963 – 965; b) G. Zhang, A. Niu, S. Peng, M. Jiang, Y. Tu, M. Li, C. Wu, *Acc. Chem. Res.* **2001**, *34*, 249 – 256.
[4] a) F. Reynolds, K. Jun, Y. Li, *Macromolecules* **2001**, *34*, 167 – 170; b) X. J. Xu, K. S. Siow, M. K. Wong, L. M. Gan, *Langmuir* **2001**, *17*, 4519 – 4524.
[5] S. Zhou, F. Yeh, C. Burger, B. Chu, *J. Phys. Chem. B* **1999**, *103*, 2107 – 2112.
[6] W. Meier, *Curr. Opin. Colloid Interface Sci.* **1999**, *4*, 6 – 14.
[7] J. Jang, K. Lee, *Chem. Commun.* **2002**, *10*, 1098 – 1099.
[8] H. Oka, M. Inagaki, Y. Kaburagi, Y. Hishiyama, *Solid State Ionics* **1999**, *121*, 157 – 163.
[9] E. Ando, S. Onodera, M. Iino, O. Ito, *Carbon* **2001**, *39*, 101 – 108.
[10] M. Inagaki, K. Fujita, Y. Takeuchi, K. Oshida, H. Iwata, H. Konno, *Carbon* **2001**, *39*, 921 – 929.
[11] F. Yan, G. Xue, M. Zhou, *J. Appl. Polym. Sci.* **2000**, *77*, 135 – 140.
[12] D. Shibuta, US Patent 5,853,877 **1996**.

Novel Capsules with High Stability and Controlled Permeability by Hierarchic Templating**

Zhifei Dai, Lars Dähne,* Helmuth Möhwald, and Brigitte Tiersch

Hollow capsules with high stability and controllable permeability have very interesting actual and potential applications, for example, as constrained environments for the preparation of nanostructured materials, the encapsulation of guest molecules, drug delivery, catalysis, and as host containers for nucleic acid storage and transport.[1,2] However, deformation and rupture of hollow capsules under shear stress may limit these applications. The stability can be increased slightly by deposition of additional layers, but the permeability decreases simultaneously. While the loading has to be fast and the release slow in most applications, the permeability of the capsules has to be tuned according to the specific application.[3] Therefore, it is desirable to develop a simple and reliable method to fabricate capsules with high stability and the desired permeability. A combination of tailorable and tunable silica nanoparticles with layer-by-layer (LbL) self-assembly[4] provides a powerful tool for the creation of exciting nanostructured systems. Silica is extremely well-suited to this purpose since well-defined particles can be prepared. Since silica is itself charged, it can be assembled with cationic polyelectrolytes, and the chemistry to dissolve it without affecting the chemical composition of the organic film components is already well established.

Here we make use of these features to prepare capsule walls of defined porosity after removal of SiO_2 (Figure 1, left) or sphere-in-sphere (SiS) structures, again after removal of SiO_2, that is sandwiched in high concentration between two indestructible walls (Figure 1, right). Similar structures can be found in nature, for example, gram-negative bacteria possess two cell walls which are separated by an aqueous phase.[5] To prepare nanoporous shells (NPS) we have used SiO_2 covered by polyallylamine hydrochloride (PAH@silica) as the cationic polyelectrolyte and polystyrene sulfonic acid (PSS) as the anionic polyelectrolyte and deposited multilayers of these by consecutive alternating adsorption on melamine formaldehyde particles (MF). The MF core is then removed by treatment with HCl, and the SiO_2 dissolved with HF. To form SiS shells, multilayers of PSS and PAH (2–3 double layers) are adsorbed alternately, followed by a variable number of silica and PAH layers (1–3 double layers) and then PSS and PAH to build-up a nondestuctable outer shell.

[*] Dr. L. Dähne, Dr. Z. Dai, Prof. H. Möhwald
Max-Planck Institute of Colloids and Interfaces
14476 Golm (Germany)
Fax: (+ 49) 30-6392-3601
E-mail: lars.daehne@capsulution.com
Dr. B. Tiersch
Department of Colloid Chemistry
Institute of Physical and Theoretical Chemistry
University of Potsdam, 14476 Golm (Germany)

[**] The authors are grateful to H. Zastrow for providing 50-nm silica particles. This work was supported by BMBF and BASF.

  0044-8249/02/4121-4019 $ 20.00+.50/0